Brain-Heart Electromechanical Modeling

Nenad Filipovic
Faculty of Engineering, University of Kragujevac
Bioengineering Research and Development Center (BioIRC)
Kragujevac, Serbia
email: fica@kg.ac.rs

Christian Helmich
TU Wien - Vienna University of Technology,
Institute for Mechanics of Materials and Structures
email: christian.hellmich@tuwien.ac.at

Jasmina Isakovic
Omnion Research International
Zagreb, Croatia
email: jasmina.isakovic@omnion-research.com

Abstract — **The brain controls the heart through the sympathetic and parasympathetic branches of the autonomic nervous system. It consists of multisynaptic pathways from myocardial cells back to peripheral ganglionic neurons and further to central preganglionic and premotor neurons. Still there are no reliable cardiovascular markers of the sympathetic tone and of the sympathetic–parasympathetic balance. It is necessary to understand interaction between brain and heart in order to make early detection and treatment of pathological changes in the brain–heart interaction.**

In this study we present a detailed electro-chemo-mechanical model for heart and torso, so as to simulate the three principal modes of actions of drugs for cardiomyopathy: (i) modulating calcium transients, (ii) changing kinetics of contractile proteins, (iii) changing the macroscopic structure or its boundary conditions. Heart model geometry included seven different regions. Monodomain model of modified FitzHugh-Nagumo model of the cardiac cell was used. Six electrodes are positioned at the chest to model the precordial leads and the results are compared with real clinical measurements. Inverse ECG method was used to optimize potential on the heart. A whole heart was embedded in the electrical activity throughout the torso environment, with spontaneous initiation of activation in the sinoatrial node, incorporating a specialized conduction system with heterogeneous action potential morphologies throughout the heart. We include body surface potential maps in a healthy subject during progression of ventricular activation in nine sequences. The electrical model was coupled with a mechanical model with orthotropic material properties obtained from experiments of Holzapfel. Future research will go more deeply in silico clinical trials where we will compare some clinical pathology and finding on the body surface with standard 12 ECG electrode measurements.

Keywords — brain-heart electrical activity, torso model, heterogeneous action potential, inverse ECG, mechanical coupling

I. Introduction

Heart-brain interaction can be understood through systems physiology, characterizing complex cardiac control mechanisms using mathematical models [1]. In particular, investigation of the effect of the baroreceptor reflex (baroreflex) on heart rate led to recording of efferent vagal activity, demonstrating that the respiratory variations in heart rate are attributable to complete stoppage of vagal efferent activity, at least in anesthetized dogs [2]. The cardiac sympathetic innervation originates from sympathetic preganglionic neurons in the upper thoracic segments of the spinal cord, which synapse with neurons in the cervical and upper thoracic ganglia. It has been demonstrated that in a variety of disease states, a high degree of parasympathetic control is correlated with improved outcome [3,4]. Sympathetic activity is also associated with ventricular repolarization heterogeneity, as indexed by T-wave alternans in subjects with coronary artery disease [5] and by QT interval variability in dogs with experimental heart failure [6].

In SILICOFCM [7] project, familial cardiomyopathy disease was modelled with comprehensive list of patient-specific features, such as genetic, biological, pharmacologic, and clinical imaging. Transport through biological barriers as vessel walls, or cell and organelle membranes, depends on the transport properties of these barriers, as hydraulic or diffusion coefficients, and also on the size of the surface which separates the continuum domains. In electrophysiology, the goal is to determine the electrophysiological properties of all compartments and signal propagation characteristics within the body. A coupled model which includes multiscale modelling of a realistic sarcomeric system, genetics patient profile, electrophysiology, realistic directions of muscle fibers, solid-fluid interaction coupled to electrophysiology of the heart was implemented. Initial results show the effect of left ventricle deformations on subsequent deformations of mitral valve, and on general blood flow in heart. Additionally, drug distribution in the heart and effects of different drugs are tested on the example of cardiomyopathy.

II. Materials and Methods

SILICOFCM project connects basic experimental research with clinical study and bioinformatics, data mining and image processing tools using very advanced computer models, and patient database and regulative in order to reduce animal and clinical studies.

The computational tools developed during the SILICOFCM project, as well as software developed prior the beginning of the SILICOFCM project by several project partners, were integrated into the SILICOFCM platform. This platform contains multiple modules that interconnect the experiments from molecular interactions to whole heart physiological function. It is an outstanding tool for supporting the drug testing. The workflow through the system is shown in Fig. 1 and the pathway through the modules connecting the experiments and supporting databases specific for each drug action is described below.

The workflow consists of three drug-testing pathways depending on the principal action of drug with different tools integrated. Specifically, each of the pathways should follow the effects of principal action of a selected drug at different scales starting from molecular interaction and their

regulation to the effects on function at the organ level. We have developed three characteristic pathways of drug flow:

(i) for drugs acting at the level of contractile proteins;

(ii) at the level of regulation of transient intracellular calcium concentration;

(iii) at the level of tissue remodeling and/or by modulation of blood vessel elasticity, i.e. resistance to blood flow and cardiac output.

These pathways are shown in Fig. 1.

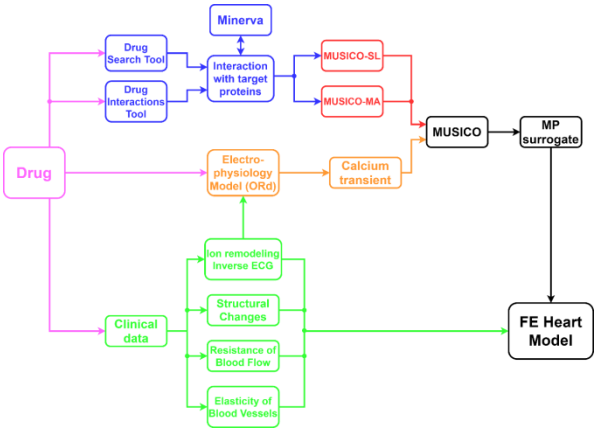

Fig. 1. Diagram of drug testing workflow in SILICOFCM.

The global architecture of the SILICOFCM drug testing workflow is shown in Fig. 1. However, the drug actions are different for the threating variety of symptoms associated with cardiomyopathies. Thus, we provided three pathways through a general workflow for different scenarios shown in Fig. 2. In particular, simulated drugs with MUSICO [8] are separated in three major groups defined by the principal action of specific drugs, as for example, on modulating calcium transients or changing kinetics of contractile proteins. Each group consists of two subgroups based on the type of cardiomyopathy:

Modulation of [Ca^{2+}] transients (Fig. 2A)

HCM – Disopyramide, which lowers peak and baseline levels of [Ca^{2+}] transient during twitch contractions [9],

DCM – Digoxin, which increases peak of [Ca^{2+}] transient during twitch contractions, but does not change time to peak and relaxation time [10],

Changes in kinetic parameters (Fig. 2B)

HCM – Mavacamten, which is associated with regulation of kinetics rates of transition between disordered myosin detached states and ordered parked state [11],

DCM – dATP, which modulates crossbridge cycle rates [12-13], Changes in macroscopic parameters (Fig. 2C)

HCM – Entresto®, which acts on remodeling of heart ventricle walls and modulates the elasticity of blood vessels, typically reducing resistance to blood flow and improving cardiac output in HCM.

Since drugs in groups 1 and 2 directly affect MUSICO [8] and MP surrogate parameters, we were able to predict with our tools the outcome on force generation in sarcomeres during twitch contractions.

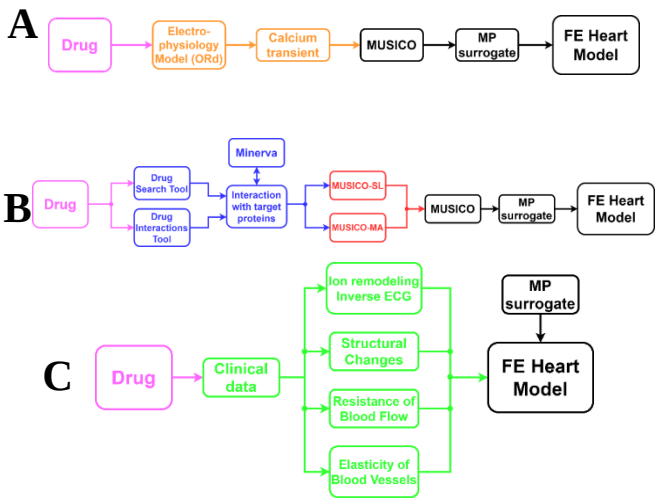

Fig. 2. Three pathways of drug action in SILICOFCM drug testing workflow. A) By modulation of calcium transient through changes in ionic currents or membrane properties, B) through changes in kinetic of contractile proteins, C) through macroscopic structural and boundary condition changes.

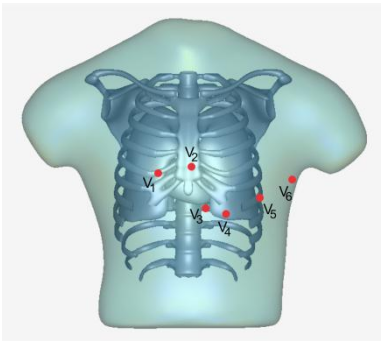

Fig. 3 Six electrodes (V1-V6) which are positioned at the chest to model the precordial leads

The electrocardiogram - ECG is a tracing of projections of cardiac electrical potentials, called leads, on specific axes, depending on probes placement. Those leads represent a view of the electrical activity of the heart from a particular angle across the body. The 12-Lead ECG became a standard in clinical practice since the American Heart Association published their recommendation in 1954. It records signals from 10 electrodes which are placed as follows (Figure 3):

- V1: 4*th* intercostal space to the right of the sternum;
- V2: 4*th* intercostal space to the left of the sternum;
- V3: midway between V2 and V4;
- V4: 5*th* intercostal space at the midclavicular line;
- V5: anterior axillary line at the same level as V4;
- V6: midaxillary line at the same level as V4 and V5;

Computer simulations were conducted using the fully coupled heart torso monodomain equations including detailed description of human ventricular cellular electrophysiology [14-15]. Myocardial and torso

conductivities were based on the literature, as presented in Table I [16-19].

TABLE I. PARAMETERS FOR MONODOMAIN MODEL WITH MODIFIED FITZHUGH-NAHUMO EQUATIONS

Parameter	SAN	Atria	AVN	His	BNL	Purkinje	Ventricles
a	-0.60	0.13	0.13	0.13	0.13	0.13	0.13
b	-0.30	0	0	0	0	0	0
c_1(AsV^{-1} m^{-3})	1000	2.6	2.6	2.6	2.6	2.6	2.6
c_2 (AsV^{-1} m^{-3})	1.0	1.0	1.0	1.0	1.0	1.0	1.0
D	0	1	1	1	1	1	1
e	0.066	0.0132	0.0132	0.005	0.0022	0.0047	0.006
A (mV)	33	140	140	140	140	140	140
B (mV)	-22	-85	-85	-85	-85	-85	-85
k	1000	1000	1000	1000	1000	1000	1000
σ ($mS{\cdot}m^{-1}$)	0.5	8	0.5	10	15	35	8

Methodology is tested with respect to a full, 3D heart model, based on linear elastic, orthotropic material model based on Holzapfel experiments [20]. Using this methodology we can accurately predict transport of electrical signals and displacement field within heart tissue. This approach has potential to be used in coupled solid-fluid simulation of whole heart in order to give accurate prediction of heart beat for different heart conditions [21].

Boundary conditions on all interior boundaries Vm, which are in contact with the torso, lungs, and cardiac cavities, are zero flux; therefore, $-\mathbf{n} \cdot \mathbf{\Gamma} = 0$ where $\mathbf{n}$ is the unit outward normal vector on the boundary and $\mathbf{\Gamma}$ is the flux vector through that boundary for the intracellular voltage, equal to $\mathbf{\Gamma} = -\sigma \cdot \partial V\text{m}/\partial \mathbf{n}$. For the variable Vm, the inward flux on these boundaries is equal to the outward current density $\mathbf{J}$ from the torso/chamber volume conductor; therefore, $-\sigma \cdot \partial V\text{m}/\partial \mathbf{n} = \mathbf{n} \cdot \mathbf{J}$.

In the second part, we implemented classical approaches for solving the ECG inverse problem using the epicardial potential formulation. The studied methods are the family of Tikhonov methods, and L regularization based methods [22-26].

ECG measurement was performed in Clinical Center Kragujevac, University of Kragujevac on the healthy volunteer.

III. RESULTS AND DISCUSSION

Here we present the electrical activity of the whole heart within the torso embedded environment, with spontaneous initiation of activation in the sinoatrial node and incorporating a specialized conduction system with heterogeneous action potential morphologies throughout the heart (Figure 4).

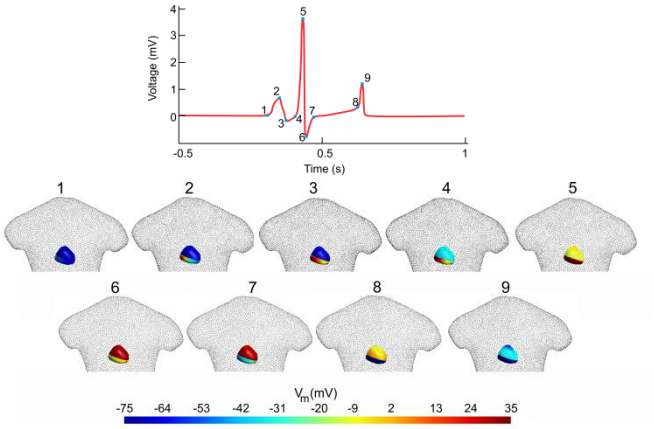

Fig. 4 Whole heart activation simulation from lead II ECG signal at various time points on the ECG signal. There are 1-9 activation sequences which are corresponding to ECG signal above. The color bar denotes mV of the transmembrane potential.

Figure 4 illustrates the simulated and measurement ECG for six electrodes (V1-V6) which are positioned at the chest to model the precordial leads for the normal heart volunteer. The normal ECG is in the agreement with standard clinical findings [27].

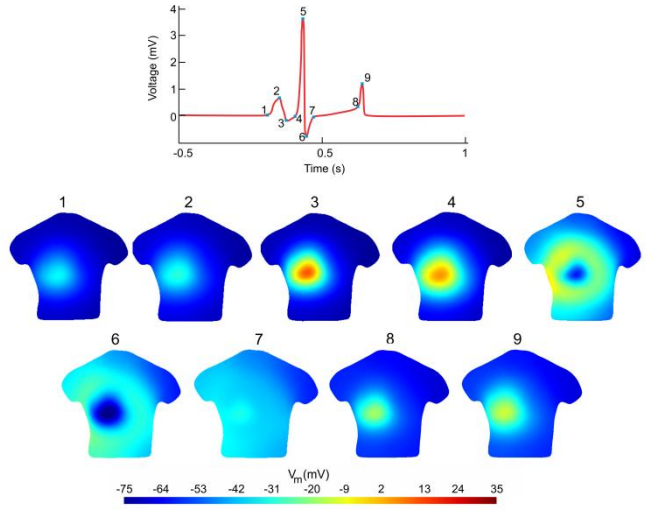

Fig 5. Body surface potential maps in a healthy subject during progression of ventricular activation in nine sequences which are corresponding to ECG signal above. The color bar denotes mV from heart activity range.

Body surface potential maps in a healthy subject during progression of ventricular activation in nine sequences which are corresponding to measurement ECG signal have been presented in Figure 5.

Boundary conditions of the mechanical model are shown in Figure 6d. Field of displacement for two different time moments of simulation, for electro-mechanical model of human heart, are shown in the Figure 6.

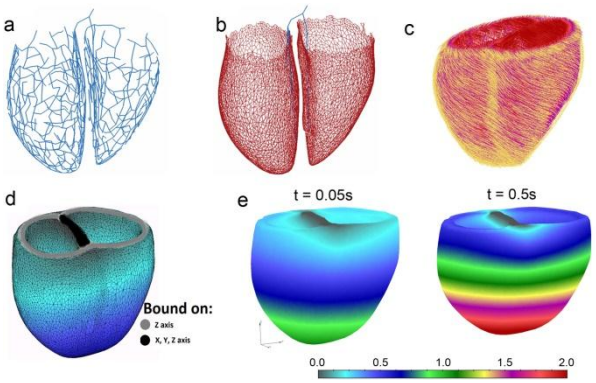

Fig. 6 Model of human heart a) Purkinje network, b) Uniform Purkinje 3D layer, c) Directions of muscle fibers, d) Boundary conditions in the model, e) Displacement field for two time moments

Using experimental data and DICOM files provided, we have reconstructed a realistic heart model as STL format with left atrium (Figure 7a, noted blue) and chamber part (Figure 7a, noted yellow) with accompanying mitral valve cross- section between (Figure 7a, noted green), and also aortic part (Figure 7a, noted orange) of the model with aortic- cross section included in fluid part of the model, which is surrounded by solid wall (Figure 7a, wireframe). Model geometry is generated using STL files. Solid nodes are constrained around inlet/outlet cross-sections. Fiber directions in solid domain of realistic heart model are shown in Figure 7b, and section c on the same figure shows distribution of velocity field in realistic heart model, at 0.1s. It can be seen that velocity values are the highest at inlet and outlet boundary cross- sections (red and green lines, Figure 7c), which is logical due to prescribed inlet function and prescribed values at that cross-section at the beginning of simulation. Regarding the material models used, we have selected Holzapfel material model [20] for obtaining passive stresses in the heart wall, and for muscle activation we used Hunter material model [22] for active stresses. Activation of the muscle is achieved using calcium function, displayed in Figure 7c.

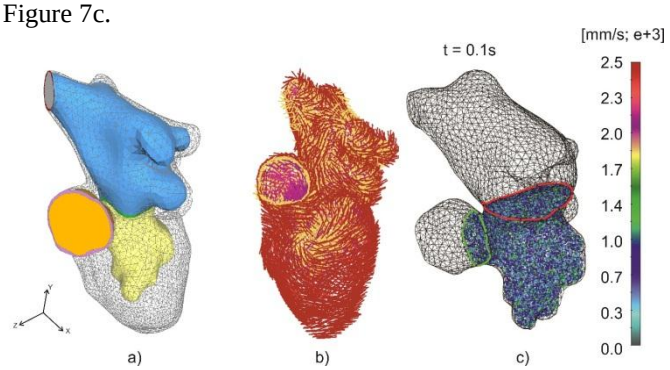

Fig. 7 a) Realistic heart FE model with representative cross- sections and fluid parts; b) Direction of fibres in solid part of realistic model; c) Fluid velocity field at 0.1s (mitral and aortic cross-section noted).

IV. Conclusion

We presented brain-heart modeling using simulated drugs for cardiomyopathy and electromechanical coupling of left ventricle and total heart in SILICOFCM [7] project. There are three major groups defined by the principal action of specific drugs: (i) modulating calcium transients, (ii) changing kinetics of contractile proteins, (iii) changing the macroscopic structure or its boundary conditions. The geometry of the heart with seven different regions of the model have been included: 1) Sinoatrial node; 2) Atria; 3) Atrioventricular node; 4) His bundle; 5) Bundle fibers; 6) Purkinje fibers; 7) Ventricular myocardium. Monodomain model of modified FitzHugh-Nagumo model of the cardiac cell was used. Six electrodes (V1-V6) are positioned at the chest to model the precordial leads and the results are compared to real clinical measurements. Inverse ECG method was used to optimize potential on the heart.

A whole heart electrical activity in the torso embedded environment, with spontaneous initiation of activation in the sinoatrial node, incorporating a specialized conduction system with heterogeneous action potential morphologies throughout the heart was presented.

Body surface potential maps in a healthy subject during progression of ventricular activation in nine sequences which are corresponding to ECG signal are presented.

We have also shown the coupling of electro model with mechanical model with linear elastic and orthotropic material model based on Holzapfel experiments.

Future research will go more deeply in silico clinical trials where we will compare some clinical pathology and finding on the body surface with standard 12 ECG electrode measurements. On a more fundamental level, the mechanical effect of non-affine fiber kinematics [28] within the vascular and neural tissues, as well as associated electro-magneto-mechanical couplings within the nervous system [29] are expected to enhance the multiscale nature of the approach, and more importantly, its clinical reliability.

Acknowledgments

The authors acknowledge support within the framework of COST Action BIONECA CA 16122 entitled “Biomaterials and Advanced Physical Techniques for Regenerative Cardiology and Neurology”.
This study is supported by the European Union’s Horizon 2020 research and innovation program under grant agreement SILICOFCM 777204 and the Ministry of Education, Science and Technological Development of the Republic of Serbia through Contracts No. 451-03-9/2021-14/200378. This article reflects only the authors’ view. The European Commission is not responsible for any use that may be made of the information the article contains.

V. References

[1] Guyton AC, Coleman TG, Cowley AW Jr, et al. Systems analysis of arterial pressure regulation and hypertension. Ann Biomed Eng 1972; 1:254–281

[2] Katona PG, Poitras JW, Barnett GO, Terry BS. Cardiac vagal efferent activity and heart period in the carotid sinus refl ex. Am J Physiol 1979; 218:1030–1037

[3] Carney RM, Freedland KE. Depression and heart rate variability in patients with coronary heart disease. Cleve Clin J Med 2009; 76(suppl 2):S13–S17

[4] Lauer MS. Autonomic function and prognosis. Cleve Clin J Med 2009; 76(suppl 2):S18–S22.

[5] Rashba EJ, Cooklin M, MacMurdy K, Kavesh N, Kirk M, Sarang S, Peters RW, Shorofsky SR, Gold MR. 2002 Effects of selective

autonomic blockade on T-wave alternans in humans *Circulation* **105**, 837–842. (doi:10.1161/hc0702.104127)

[6] Piccirillo G *et al.* 2009 Autonomic nervous system activity measured directly and QT interval variability in normal and pacing-induced tachycardia heart failure dogs. *J. Am. Coll. Cardio* **54**, 840–850. (doi:10.1016/j.jacc.2009.06.008)

[7] www.silicofcm.eu

[8] https://www.solindies.com/musico

[9] Coppini, R., Ferrantini, C., Pioner, J. M., Santini, L., Wang, Z. J., Palandri, C., ... & Sherrid, M. V. (2019). Electrophysiological and contractile effects of disopyramide in patients with obstructive hypertrophic cardiomyopathy: a translational study. JACC: Basic to Translational Science, 4(7), 795-813.

[10] Morgan, J. P., Chesebro, J. H., Pluth, J. R., Puga, F. J., & Schaff, H. V. (1984). Intracellular calcium transients in human working myocardium as detected with aequorin. Journal of the American College of Cardiology, 3(2), 410-418.

[11] Ma, W., Marcus, M., Anderson, R. L., Gong, H., Wong, F. L., del Rio, C. L., Irving, T. The super-relaxed state and length dependent activation in porcine myocardium. (in press).

[12] Regnier, M., Lee, D. M., & Homsher, E. (1998). ATP analogs and muscle contraction: mechanics and kinetics of nucleoside triphosphate binding and hydrolysis. Biophysical journal, 74(6), 3044-3058.

[13] Regnier, M., Rivera, A. J., Chen, Y., & Chase, P. B. (2000). 2-deoxy-ATP enhances contractility of rat cardiac muscle. Circulation research, 86(12), 1211-1217.

[14] C. A. Gibbons Kroeker, S. Adeeb, J. V. Tyberg, and N. G. Shrive, "A 2D FE model of the heart demonstrates the role of the pericardium in ventricular deformation", *American Journal of Physiology*, vol. 291, no. 5, pp. H2229–H2236, 2006.

[15] A. J. Pullan, M. L. Buist, and L. K. Cheng, *Mathematically Modelling the Electrical Activity of theHeart—FromCell To Body Surface and Back Again*,World Scientific, 2005.

[16] M.-C. Trudel, B. Dub´e, M. Potse, R. M. Gulrajani, and L. J. Leon, "Simulation of QRST integral maps with a membrane based computer heart model employing parallel processing", *IEEE Transactions on Biomedical Engineering*, vol. 51, no. 8, pp. 1319–1329, 2004.

[17] M. Wilhelms, O. Dossel, G. Seemann, "In silico investigation of electrically silent acute cardiac ischemia in the human ventricles". *IEEE Trans Biomed Eng* 58, 2961–4, 2011.

[18] R. Fitzhugh, "Impulses and physiological states in theoretical models of nerve membrane". Biophysical J., 1: 445-466, 1961.

[19] J. Nagumo, S. Arimoto, S. Yoshizawa, "An active pulse transmission line simulating nerve axon". *Proc. IRE*., 50: 2061-2070, 1962.

[20] G. A. Holzapfel. Determination of material models for arterial walls from uniaxial extension tests and histological structure. Journal of Theoretical Biology, Elsevier, 2006, 10.1016/j.jtbi.2005.05.006. hal-01299856

[21] S. Sovilj, R. Magjarević. N. Lovell, S. Dokos, " A simplified 3D model of whole heart electrical activity and 12-lead ECG generation". *Computational and Mathematical Methods in Medicine*, doi:10.1155/2013/134208, 2013.

[22] M. Kojic, M. Milosevic V. Simic, B. Milicevic, V. Geroski, S. Nizzero, A. Ziemys, N. Filipovic, M. Ferrari, "Smeared Multiscale Finite Element Models for Mass Transport and Electrophysiology Coupled to Muscle Mechanics", *Frontiers in Bioengineering and Biotechnology*, ISSN 2296-4185, Vol. 7, 381, pp. 1-16, 2296-4185, 2019.

[23] Y. Wang, and .Y Rudy, "Application of the method of fundamental solutions to potential-based inverse electrocardiography". Annals of biomedical engineering 34, 8, 1272–1288, 2006.

[24] A. Van Oosterom, "The use of the spatial covariance in computing pericardial potentials". *IEEE Transactions on biomedical engineering* 46, 7, 778–787, 1999.

[25] A. Van Oosterom, "The spatial covariance used in computing the pericardial potential distribution". *Computational Inverse Problems in Electrocardiography*, 1–50, 2001

[26] A. Van Oosterom,"Source models in inverse electrocardiography". *Int J Bioelectromagn* 5 211–214, 2003.

[27] A. Van Oosterom, "The equivalent double layer: source models for repolarization". *In Comprehensive Electrocardiology*. Springer, pp. 227–246., 2010.

[28] C. Morin, S Avril, Ch Hellmich. Non-affine fiber kinematics in arterial mechanics: a continuum micromechanical investigation. *ZAMM - Zeitschrift für Angewandte Mathematik und Mechanik* 98, pp. 2101–2121, 2018.

[29] J. Isakovic, I. Dobbs-Dixon, D. Chaudhury, D. Mitrecic, Modeling of inhomogeneous electromagnetic fields in the nervous system: a novel paradigm in understanding cell interactions, disease etiology and therapy. *Scientific Reports* 8, 12909, 2018.